

3.3 SATELLITE-BASED TROPICAL CYCLONE INTENSITY ESTIMATION USING THE NOAA-KLM SERIES ADVANCED MICROWAVE SOUNDING UNIT (AMSU):

Kurt F. Brueske¹
And
Christopher S. Velden

University of Wisconsin – CIMSS, Madison, Wisconsin, USA

1. Introduction

The 2001 northern hemisphere hurricane season marks the third year of passive microwave warm core observations using the NOAA-KLM series Advanced Microwave Sounding Unit (AMSU). Over the past two decades, several authors (Kidder et al., 1978, Velden et al., 1991, Kidder et al., 2000) have documented the virtues of monitoring tropical cyclone (TC) intensity using satellite-borne passive microwave radiance data. In summary, 55GHz region microwave observations of TC upper tropospheric warm anomalies (UTWA) are linked to wind structure and minimum sea level pressure (MSLP) using thermodynamic and dynamic constraints on the TC scale (i.e., several hundred km).

composite aircraft and radiosonde observation data in the late 1960s (Koteswaram, 1967).

In a novel simulation study, Merrill (1995) introduced the concept of passive microwave radiometer observation “effective accuracy” and demonstrated that, for a variable horizontal resolution instrument like the NOAA-KLM AMSU-A, the TC UTWA resolving limit is a non-linear function of several time-variant parameters including:

- AMSU-A scan angle (ϕ)
- AMSU-A scan angle off-axis angle (θ)
- UTWA horizontal scale (R)
- Scattering by mixed-phase hydrometeors

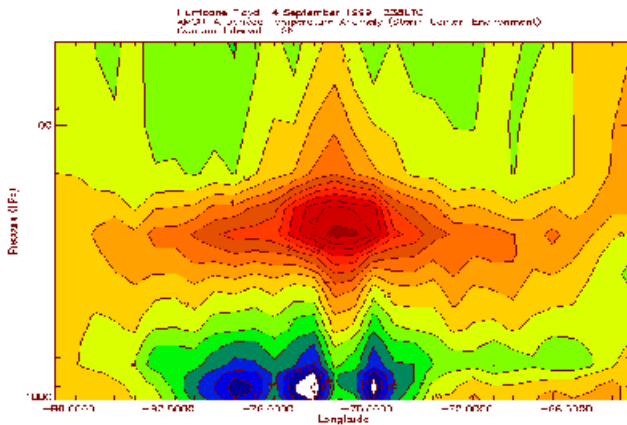


Figure 1. Hurricane Floyd 14 Sep 1999 1238UTC temperature anomaly derived from AMSU-A radiance data. An UTWA of approximately 18°C was observed at 250hPa. Aircraft reconnaissance reported a MSLP value of 924hPa at 1113UTC.

Recently, temperature profiles constructed using AMSU-A multi-spectral observations and the National Oceanic and Atmospheric Administration (NOAA) National Environmental Satellite Data Information Service (NESDIS) retrieval algorithm (Fig. 1) have produced TC warm core vertical cross sections strikingly similar to the classic profiles derived from

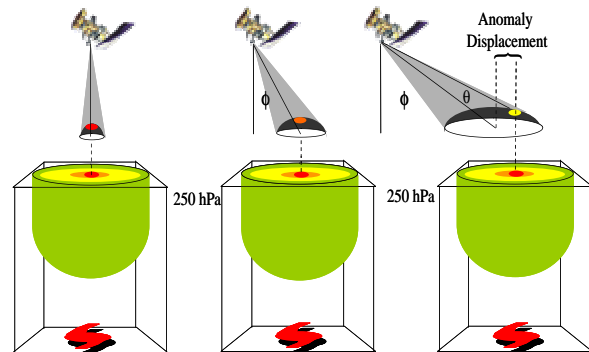


Figure 2. A schematic diagram illustrating AMSU-A horizontal resolution as a function of scan angle (ϕ) and off-axis angle (θ) for a mature TC. Note the difference in size between nadir and limb FOV.

Due to the ephemeral nature of TC position (ϕ, θ) and UTWA horizontal scale (R) between successive AMSU-A observations (Fig. 2), there exists a non-zero component of the UTWA temporal variability that is purely instrument related vs. change that reflects actual thermodynamic (and TC intensity) structure change. The end result is fictitious temporal UTWA variability and smoothing that can introduce error in schemes that

¹ Corresponding author address: Kurt F. Brueske, Capt, USAF, PhD, United States Air Force Academy Department of Physics, Suite 2A211 Fairchild Hall USAF Academy CO 80840

attempt to statistically relate 55GHz-region passive microwave UTWA observations with TC MSLP. The aforementioned effects are non-trivial and have limited past attempts to develop and implement satellite-based TC passive microwave intensity estimation techniques.

The remainder of this paper describes the development, test and evaluation of an algorithm designed to explicitly model and remove undesirable TC scale and AMSU-A instrument scan geometry effects according to the methodology prescribed by Merrill (1995). Section 2 describes the satellite data and in-situ observations used in this study followed by a description of the salient features of the maximum likelihood retrieval algorithm in Section 3. Section 4 describes the results of a fully automated, independent test in 2000 where TC MSLP was diagnosed using raw and scan geometry-corrected (hereafter referred to as retrieved) UTWA information derived from limb-corrected AMSU-A 54.94GHz brightness temperature data followed by a brief discussion of factors that limit AMSU TC intensity estimate accuracy. Section 5 provides a summary and briefly describes ongoing technology transition and future research activities. Acknowledgements and references are provided in Sections 6 and 7.

2. Data

Global AMSU-A/B earth observation radiance data is forwarded by NOAA/NESDIS to the University of Wisconsin-Madison (UW) Space Science and Engineering Center (SSEC) Cooperative Institute for Meteorological Satellite Studies (CIMSS) for near real-time processing and archival. Average time delays between AMSU TC observation and SSEC/CIMSS receipt range from 1-3 hours based on several factors including TC location, NOAA/NESDIS internal processing schedules, telecommunications network activity, etc. Only under extreme circumstances does the time delay exceed 3 hours.

Development of the 1999 dependent data set required the identification and manual retrieval of NOAA-15 AMSU-A/B orbits providing TC coverage. Visualization of orbit coverage (near-real time and post-event) and determination of precise TC overpass time (UTC) were made possible using the UW-SSEC Man-computer Interactive Data Access System (McIDAS). Relevant AMSU-A/B orbit files were then acquired from a local UW-CIMSS near real-time archive or restored from 8mm tape. The entire navigation/acquisition process was automated in support of the 2000 independent test, as well as for future research and development activities, and is discussed in more detail in Section 4. Radio frequency interference with NOAA-15 AMSU-A and AMSU-B instruments prohibited the consideration of TC data in 1998.

Atlantic and eastern Pacific basin TC reconnaissance observations from the United States Air Force Reserve 53rd Weather Reconnaissance Squadron and NOAA were used to (1) develop dependent test regression coefficients relating raw/retrieved AMSU-A UTWA magnitudes to aircraft reconnaissance estimates of MSLP and (2) validate independent test results. The

selection of AMSU-A/aircraft reconnaissance "pairs", for both dependent and independent samples, were based on the time difference between aircraft reconnaissance and AMSU-A observations and environmental conditions. Only those observations that occurred within +/- 6 hrs of each other and for which the TC was not undergoing significant intensity change due to interaction with land, wind shear, etc. were considered.

3. Forward Model

As discussed in Section 1, AMSU-A horizontal resolution varies from approximately 48km near satellite nadir to over 100km near scan limb. The combined effects of subsidence and high inertial stability within the inner-eyewall region constrain the horizontal dimensions of peak TC UTWA warming to scales less than even the most optimal AMSU-A viewing conditions (i.e., $\phi = 0^\circ, \theta = 0^\circ$). As a result, the true magnitude of TC UTWAs will typically be sub-sampled for all but a small minority of TCs possessing large eyes (and corresponding UTWA horizontal scales) or average sized systems that happen to fall fortuitously near center of an AMSU-A FOV near satellite nadir. In reality, TCs are characterized by a wide variety of horizontal scales and are free to fall anywhere within the AMSU-A scan swath; therefore, knowledge of the effects of storm scale (R) and scan geometry (ϕ, θ) are vital steps towards TC UTWA optimization and MSLP estimate accuracy.

The approach used in this study is based on the methodology proposed by Merrill (1995) using previous generation Microwave Sounding Unit (MSU) data. Adopting Merrill's technique for use with AMSU-A, the observed 54.94GHz horizontal brightness temperature distribution $B^{obs}(x,y)$, from which the TC UTWA is estimated, is considered a convolution of the true upper tropospheric thermal distribution $B^{true}(x,y)$ and the antenna gain pattern $F(x,y,\nu)$ (Fig. 3).

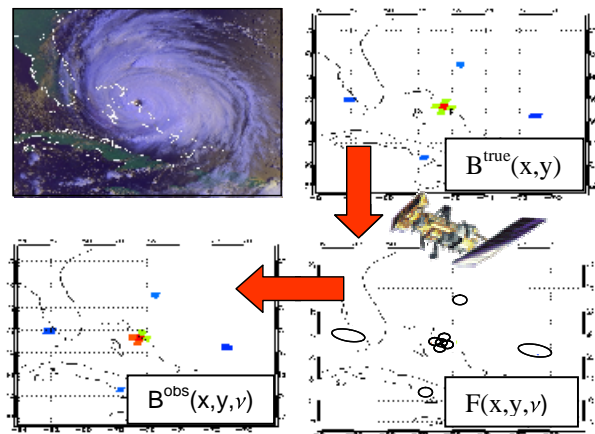


Figure 3. A schematic diagram illustrating the concept of true TC UTWA convolution with the AMSU-A antenna gain pattern for Hurricane Floyd 14 Sep 1999 1238UTC. AVHRR multi-spectral image (inset) courtesy of Dave Santek, UW-SSEC.

This can be represented mathematically as:

$$B^{\text{obs}}(x,y,\nu) = B^{\text{true}}(x,y)F(x,y,\nu)dA \quad (1)$$

assuming that (1) the atmosphere is sufficiently opaque at $\nu = 54.94\text{GHz}$ such that the surface emission term can be neglected, (2) the frequency-dependent weighting function does not vary significantly over the depth of layer atmospheric layer characterized by the peak upper tropospheric warming, and (3) scattering by mixed-phase hydrometeors is negligible (see Section 4). The antenna gain pattern $F(x,y,\nu) \sim F(\phi,\theta,\nu)$ for off-nadir scan angle ϕ is uniquely prescribed based on the diffraction pattern of a uniformly illuminated circular aperture:

$$F(\phi,\theta,\nu) \sim 4\{J_1(\nu d \sin \theta) / \nu d \sin \theta\}^2 \quad (2)$$

where J_1 is a Bessel function (first kind, order one), ν is the frequency of incident radiation (54.94GHz), d is the AMSU-A instrument bore sight aperture (m), and θ is the scan angle off-axis angle defined by the displacement of the TC LLCC from the center of the AMSU-A FOV containing the peak UTWA warming (Fig. 2). Finally, dA represents the area formed by the intersection of the AMSU-A antenna gain pattern with the earth's surface (see Fig. 3).

Assuming that the TC is in hydrostatic balance at the storm scale, the true upper tropospheric thermal distribution $B^{\text{true}}(x,y,\nu)$ is assumed to mirror the surface pressure distribution. As a result, the form of $B^{\text{true}}(x,y)$ is modeled after Holland (1980):

$$B^{\text{true}}(x,y) \sim B(x,y,\mathbf{X}) = B_{\text{env}} + \Delta_B \{1 - e^{-(R/r)^\gamma}\} + B_x(x-x_c) B_y(y-y_c) \quad (3)$$

where B_{env} represents undisturbed environmental conditions, Δ_B the UTWA magnitude for a mature TC, B_x and B_y the environmental derivatives (longitude and latitude), x and y the position relative to TC center (x_c, y_c) , and $r = (|x - x_c|^2 + |y - y_c|^2)^{1/2}$. The term within curly brackets $\{\}$ defines the shape of the radial distribution of the UTWA as a function of distance r from the TC center. R , which represents the UTWA horizontal scale, is a vital component of (3) and must be prescribed accurately in order to maximize the representativeness of $B^{\text{true}}(x,y)$ in the forward model. γ is a dimensionless shape factor that describes the eccentricity of the UTWA.

\mathbf{X} represents a tunable TC UTWA horizontal structure function (column vector) consisting of 8 parameters

$$\mathbf{X} = [B_{\text{env}}, \Delta_B, R, \gamma, B_x, B_y, x_c, y_c]^T \quad (4)$$

all of which, with the exception of R , x_c and y_c , are initially assigned constraint (\mathbf{X}^{con}) a-priori mean values

and error variances based on satellite or aircraft reconnaissance-derived parameter climatologies (Merrill, 1995). In this study, the TC UTWA size parameter R is defined through the spatial analysis of AMSU-B 89.0GHz moisture sounder window channel radiance data (Fig. 4). AMSU-B 89.0GHz radiances are strongly attenuated by convection within the TC eye wall region (Kidder et al., 2000) and are therefore used as a proxy for eye size. An interpolating polynomial $F(r)$ is fit to the radial distribution of AMSU-B 89.0GHz radiance data and R is assumed to occur at $|d^2F(r)/dr^2| = 0$ (inflection point) coincident with reduced AMSU-B 89.0GHz brightness temperatures characteristic of convective hydrometeor scattering within the eye wall region. The final R value is found by averaging up to

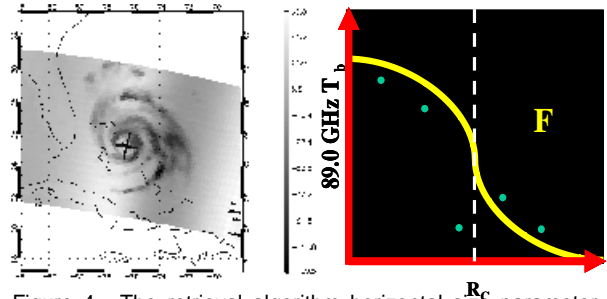


Figure 4. The retrieval algorithm horizontal size parameter (R) is determined through spatial analysis of AMSU-B 89.0GHz radiance data. In this example, TC position for Hurricane Floyd, 14 Sep 1999 1238UTC (left) is specified and an interpolating polynomial function $F(r)$ is defined in each of four total directions (right) in image array line/element. Hydrometeor scattering within the eye wall region is used as an indicator of eye size itself a proxy for UTWA horizontal scale.

four separate R estimates from each radial direction in AMSU-B radiance array line/element space. For the development of the 1999 dependent sample, TC position (x_c, y_c) was determined using published forecast position bulletins generated by the National Hurricane Center (NHC) and Navy/Air Force Joint Typhoon Warning Center (JTWC) with fine scale adjustments based on the visual inspection of AMSU-B 89.0GHz data.

Once the constraint structure vector \mathbf{X}^{con} (4) is specified, it is used by the forward model to estimate the expected radiance distribution $B_m^{\text{fwd}}(x,y,\mathbf{X}_m)$ where \mathbf{X}_m is the m -th iterated storm structure vector. This process is repeated until the difference between the observed AMSU-A radiance distribution $B^{\text{obs}}(x,y,\nu)$ and $B_m^{\text{fwd}}(x,y,\mathbf{X}_m)_{m \rightarrow \infty}$ are minimized. At each iterative step, \mathbf{X}_m is perturbed according to the method proposed by Rodgers (1976):

$$\mathbf{X}_{m+1} = \mathbf{X}^{\text{con}} + \mathbf{S}_{\text{xx}}^{\text{con}} \mathbf{K}_m^T (\mathbf{K}_m \mathbf{S}_{\text{yy}}^{\text{con}} \mathbf{K}_m^T + \mathbf{S}_{\text{yy}})^{-1} [\mathbf{Y}^{\text{obs}} - \mathbf{Y}_m - \mathbf{K}_m (\mathbf{X}^{\text{con}} - \mathbf{X}_m)] \quad (5)$$

where \mathbf{X}^{con} is the constraint (a priori) storm structure vector, $\mathbf{S}_{\text{xx}}^{\text{con}}$ the constraint structure error covariance, \mathbf{K}_m the forward model sensitivity to changes in the

structure vector (i.e., $\partial B_m^{fwd}(x,y, X_m)/\partial X_m$), and S_{yy} the AMSU-A observation error covariance. Based on (5), the maximum likelihood solution for the storm structure function $X^{ret}(X_m, m \rightarrow 8)$, including the retrieved UTWA (ΔB^{ret}), occurs when the differences between the observed AMSU-A radiances B^{obs} and forward model radiances B_m^{fwd} and the forward model sensitivity-weighted difference between the constraint storm structure X^{con} and m-th iteration structure X_m are the same. Finally, the scan-geometry and diffraction-corrected UTWA (ΔB^{ret}) is retrieved through inversion of the solution structure function X^{ret}

$$\Delta B^{ret} = [X^{ret}]^{-1} \quad (6)$$

The ability of the retrieval algorithm (5) to resolve X^{ret} , and therefore ΔB^{ret} , depends highly on the accuracy of the constraint storm structure X^{con} . As noted by Merrill (1995), the solution storm structure X^{ret} will always fall between X^{con} and the value of X that best produces the AMSU-A observed radiance distribution B^{obs} . Whether the actual AMSU-A observation or constraint is favored depends upon the expected constraint structure error covariance S_{xx}^{con} , the expected observation variance (noise) S_{yy} , and the sensitivity of the forward model to changes in the storm structure K_m . $S_{xx}^{con} \rightarrow 0$ implies that X^{con} is a good estimate of the storm structure and the solution will favor the constraint with zero variance. On the other hand, $S_{xx}^{con} \rightarrow 8$ implies X^{con} is a poor estimate of the storm structure and the solution tends toward the inversion of the forward model. S_{yy} and K_m are coupled in the sense that accurate AMSU-A observations (i.e., $S_{yy} \rightarrow 0$) or large forward model sensitivities K_m (i.e., favorable viewing geometry \rightarrow satellite nadir, FOV centered) cause the solution to favor the solution of the forward model whereas $S_{yy} \rightarrow 8$ or small K_m (i.e., unfavorable view geometry \rightarrow satellite limb, non FOV-centered) favor the constraint X^{con} .

During 1999, 22 cases in the Atlantic/Eastern Pacific Basin satisfied the criteria specified in Section 2 and were used to develop the dependent sample. Three parallel tests were conducted using identical NOAA-15 AMSU-A and in-situ MSLP data sets (Fig. 5). The first test (red) related the raw AMSU-A 54.94GHz derived UTWA (ΔB) with in-situ MSLP estimates while the other two tests related the retrieved UTWA (ΔB^{ret}) with in-situ MSLP estimates after explicitly treating and removing the scan-geometry and diffraction effects. Of the two tests in which the retrieval algorithm was applied, one used a fixed climatological horizontal scale parameter (green) of 24km (Weatherford and Gray, 1988) while the other test (blue) used variable R values derived using AMSU-B 89.0GHz radiance data. The test results demonstrate that while a moderate degree of correlation ($R^2 \sim 0.70$) exists naturally between ΔB and MSLP, a significantly higher degree of correlation ($R^2 \sim 0.90$) between ΔB^{ret} and MSLP is possible using the retrieval and AMSU-B 89.0GHz radiance data. The relatively similar performance between ΔB^{ret} vs. MSLP (R fixed) and ΔB^{ret} vs. MSLP (R variable) likely reflects

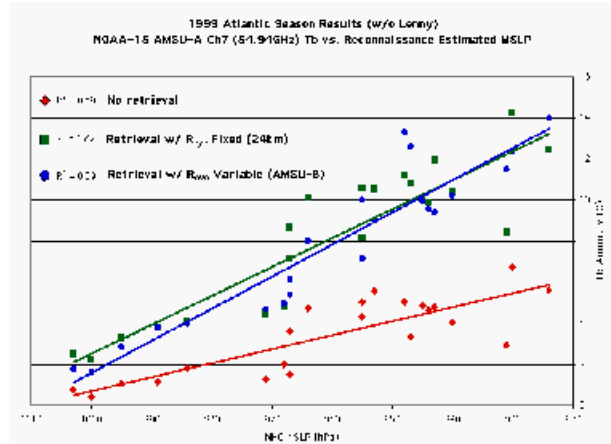


Figure 5. Results of the 1999 dependent test. Application of the retrieval increases the resolved UTWA and improves correlation with MSLP determined by aircraft.

the similarity in sizes between climatological R values and the average of those derived from AMSU-B 89.0GHz data ($R_{ave}^{89.0GHz} = 22.4km$). In summary, the results of the dependent test – increased UTWA resolution and improved correlation with reconnaissance MSLP estimates – validate Merrill’s earlier hypothesis on TC UTWA sub sampling and strongly support the need for application of the retrieval algorithm.

4. Independent Test

Based on the results of the dependent test in 1999, an automated processing scheme was devised (Fig. 6) to diagnose MSLP in 2000 using solely ΔB , ΔB^{ret} and regression coefficients derived

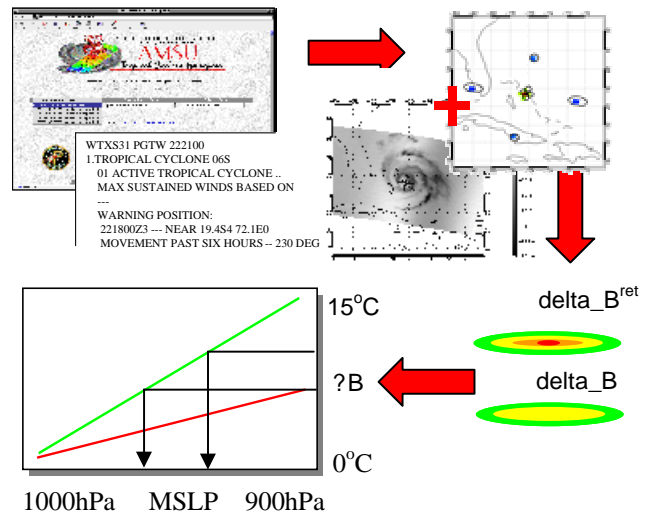


Figure 6. A schematic of the automated AMSU TC MSLP estimate processing routine executed during the independent test. Steps 1-4 are clock-wise starting in the upper left corner.

from the 1999 dependent sample. Processing was “event-driven” based on TC position estimates

published within NHC/JTWC forecast discussion bulletins (Step 1). Based on TC position, AMSU-A/B observation data was acquired, the size parameter R determined, and the forward model run using AMSU-A FOV scan angles (ϕ) and off-axis angles (θ) (Step 2) leading to estimates of the raw (Δ_B) and retrieved (Δ_B^{ret}) UTWA (Step 3). During the final step (Step 4), TC MSLP was diagnosed using the following dependent data set linear least squares regression equations:

$$\begin{aligned} \text{MSLP}_{\text{ret}} &= (150.7 - \Delta_B^{\text{ret}}) / 0.15 \\ \text{MSLP}_{\text{raw}} &= (65.4 - \Delta_B) / 0.07 \end{aligned} \quad (7)$$

Overall, the independent test in the Atlantic and eastern Pacific basins was a success and further reinforced the prior dependent test results. A total of 31 cases met the selection criterion discussed in Section 2. The retrieval yielded Δ_B^{ret} values (green) more highly correlated with reconnaissance estimates of MSLP than did Δ_B (red) ($R^2=0.95$ vs. 0.80) and AMSU-based MSLP estimate mean error and standard deviations were also smaller using the retrieval (6.2hPa +/- 8.0hPa vs. 7.5hPa +/- 9.9hPa). In addition, the independent test results performed admirably in a homogenous comparison with Dvorak (1975) intensity estimates (7.8hPa +/- 7.6hPa) generated by the NOAA Satellite Analysis Branch (SAB) and Air Force Weather Agency (AFWA). Fig. 7 illustrates the combined 1999/2000

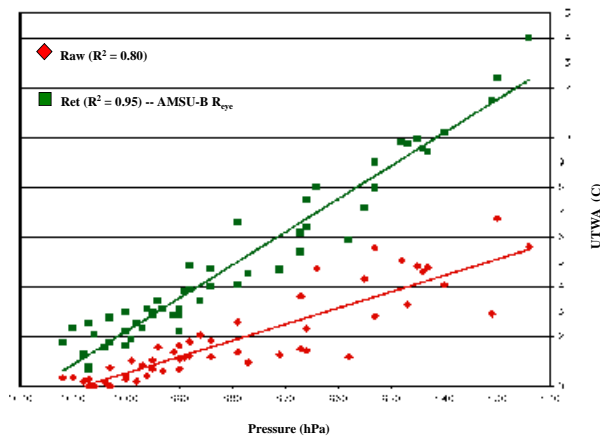


Figure 7. Combined 1999/2000 results. Year 2000 results reinforce earlier findings of the dependent test and further support the linear relationship between true UTWA strength and TC MSLP.

results (n=53). It is noteworthy that application of the retrieval algorithm further reinforces the linearity between satellite-borne 55GHz region passive microwave observations of TC UTWAs and MSLP.

After applying the AMSU TC MSLP retrieval algorithm over the past two years – the first year to train the algorithm followed by the independent test year --

several factors emerged that affect retrieval performance including (1) determination of TC position at the time of AMSU observation, (2) estimating eye size (radius) using AMSU-B 89.0GHz radiance data – particularly near the scan limb, and (3) hydrometeor scattering associated with deep convection in the inner eye wall region. Two years worth of AMSU-A TC observations suggests that the issue of 55GHz region scattering, assumed negligible in Eqn. 1 (Section 3), is occasionally violated particularly during periods when exceptionally deep convection (e.g. convective bursts) occurs close to the LLCC of a TC. Under these circumstances, AMSU-A 54.94GHz radiances can be attenuated (Fig. 8) and any attempt to determine the magnitude of the UTWA (now a cold anomaly) will lead to erroneous TC MSLP estimates.

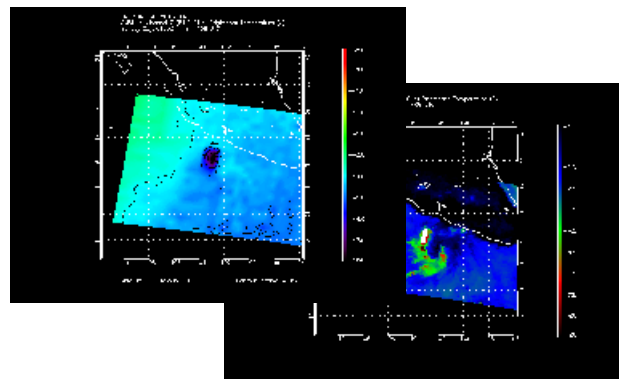


Figure 8. An example of the impact of a convective burst and hydrometeor scattering on AMSU-A 54.94GHz radiance data (left) for Tropical Storm Dalila 22 Jul 2001 1408UTC. The corresponding AMSU-B 89.0GHz image is provided (right).

Another leading factor that limited AMSU TC MSLP estimate accuracy during the independent test was the ability (or inability) of the algorithm to determine TC eye size (R) using AMSU-B 89.0GHz radiance data. As mentioned in Section 3, optimization of the constraint horizontal structure function X^{con} is absolutely critical to the retrieval algorithm performance. In its current form, R estimates require relatively precise TC positioning at the time of AMSU observation. Based on differences between published NHC/JTWC initial position and motion estimates and the time of AMSU observation, TC position is adjusted using linear extrapolation. In circumstances where TC extrapolated position is inaccurate, the quality of R estimates will be reduced and the performance of the retrieval and MSLP estimates will suffer accordingly. Any number of factors, often in combination, contribute to this problem including 1) poorly defined TCs (e.g., genesis stage, systems undergoing shearing, etc.) where determination of position using visible/infrared satellite imagery is difficult, 2) TCs characterized by high uncertainty in short-term motion/track, and 3) cases with large time differences between forecasting center initial position estimates and AMSU TC observation.

5. Summary and Future Research

Passive microwave radiometers like the AMSU provide a unique opportunity to monitor and assess changes in TC intensity based on observed changes in UTWA structure. By implementing a maximum likelihood regression technique first proposed by Merrill (1995), the authors have successfully demonstrated that the adverse effects of variable sensor horizontal resolution, storm scan geometry, and diffraction effects can be explicitly modeled and removed. Furthermore, AMSU TC UTWA values produced by the retrieval yielded superior TC MSLP estimates compared to those generated using raw UTWA observations, reducing both mean MSLP estimate error and variance. Finally, the similarity in performance between AMSU and Dvorak (1975) intensity estimates Dvorak technique substantiates the value of the AMSU as a future TC intensity estimation tool.

In 2001, the UW-CIMSS, in cooperation with the USAF and Naval Research Laboratory-Monterey, is generating near real-time AMSU TC MSLP estimates using an automated, objective, web-based approach similar to the method exercised internally at UW-CIMSS in 2000. The software suite, in its current form, is capable of supporting up to 5 simultaneous TCs in 4 geographically separate basins (Atlantic, Eastern Pacific, Western Pacific (Northern and Southern Hemisphere), and Indian Ocean (Northern and Southern Hemisphere)) with minimal human intervention. Near real-time AMSU TC imagery products are available to a global audience via the world-wide-web at <http://amsu.ssec.wisc.edu>. AMSU TC MSLP estimates are also being forwarded to NHC, JTWC, NOAA/SAB and AFWA for evaluation and feedback.

Several initiatives and enhancements are undergoing immediate development or are in the process of being planned in the near future. These include:

- A multiple channel regression approach using multiple AMSU-A tropospheric channels
- A web-based manual retrieval interface that allows client specification of TC position and R
- AMSU 'INVEST' processing coupled with NRL-MRY and ATCF
- Extension of the retrieval algorithm for use with DMSP SSMIS
- AMSU-A based hydrostatic eye sounding corrected for precipitation (scattering) effects

all of which will improve our ability to monitor and assess TC intensification and environmental interaction.

6. Acknowledgements

We gratefully acknowledge the support of our research sponsors, the Office of Naval Research, Program Element (PE-060223N), the Space and Naval Warfare Systems Command, PMW-155 (PE-0603207N), the Naval Research Laboratory (Jeff Hawkins), and the United States Air Force Academy

Department of Physics (USAFA/DFP). The authors would also like to recognize Dr. Robert T. Merrill (formerly of UW-CIMSS) for his pioneering contributions towards the development of the original XTCR algorithm upon which this research is based. Finally, the authors would like to thank the USAF 53rd WRS, NOAA/NESDIS, USAF Weather Agency, and the Australian Bureau of Meteorology for making available timely TC in situ observation data in near real-time.

7. References

Dvorak, V. F., 1975: Tropical cyclone intensity analysis and forecasting from satellite imagery. *Mon. Wea. Rev.*, **103**, 420-430.

Holland, G. J., 1980: An analytic model of the wind and pressure profiles in hurricanes. *Mon. Wea. Rev.*, **108**, 1212-1218.

Kidder, S. Q., Gray, W. M., and T.H. Vonder Haar, 1978: Estimating Tropical Cyclone Central Pressure And Outer Winds From Satellite Microwave Sounder Data. *Mon. Wea. Rev.*, **108**, 1458-1464.

Kidder, S.Q., M.D. Goldberg, R.M. Zehr, M. DeMaria, J.F.W. Purdom, C.S. Velden, N.C. Grody, and S.J. Kusselson, 2000: *Bull. Amer. Meteor. Soc.*, **81**, 1241-1259.

Koteswaram, P., 1967: On The Structure Of Hurricanes In The Upper Troposphere And Lower Stratosphere. *Mon. Wea. Rev.*, **95**, 541-564.

Merrill, R.T., 1995: Simulations of Physical Retrieval of Tropical Cyclone Thermal Structure Using 55 GHz-Band Passive Microwave Observations from Polar-Orbiting Satellites. *J. App. Meteor.*, **34**, 774-787.

Rodgers, C. A., 1976: Retrieval of atmospheric temperature and composition from remote measurements of thermal radiation. *Rev. Geophys. Space Phys.*, **14**, 609-624.

Simpson, J., 2000: Personal communication.

Velden, C. S., Goodman, B. M., and R. T. Merrill, 1991: Western North Pacific Tropical Cyclone Intensity Estimation from NOAA Polar-Orbiting Satellite Microwave Data. *Mon. Wea. Rev.*, **119**, 159-168.

Weatherford, C. L., and W. M. Gray, 1988: Typhoon structure as revealed by aircraft reconnaissance. Part I: Data analysis and climatology. *Mon. Wea. Rev.*, **116**, 1032-1043.

This document was created with Win2PDF available at <http://www.daneprairie.com>.
The unregistered version of Win2PDF is for evaluation or non-commercial use only.